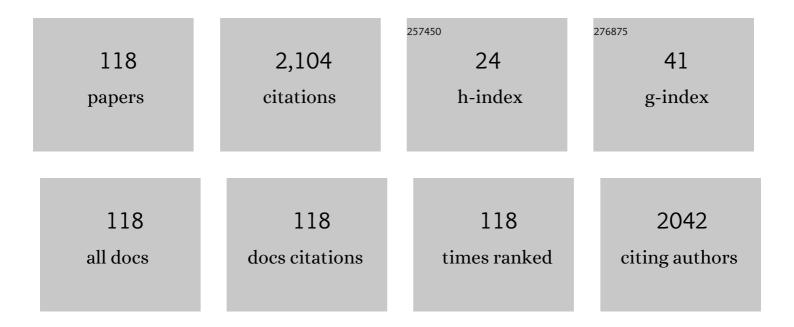
Katsuhiko Saito

List of Publications by Year in descending order

Source: https://exaly.com/author-pdf/9606148/publications.pdf Version: 2024-02-01



#	Article	IF	CITATIONS
1	Wide bandgap engineering of (AlGa)2O3 films. Applied Physics Letters, 2014, 105, .	3.3	161
2	Influence of composition ratio on properties of Cu2ZnSnS4 thin films fabricated by co-evaporation. Thin Solid Films, 2010, 518, S29-S33.	1.8	155
3	Structural and optical properties of Ga2O3 films on sapphire substrates by pulsed laser deposition. Journal of Crystal Growth, 2014, 387, 96-100.	1.5	134
4	Existence and removal of Cu2Se second phase in coevaporated Cu2ZnSnSe4 thin films. Journal of Applied Physics, 2012, 111, .	2.5	87
5	Electrical properties and emission mechanisms of Zn-doped β-Ga2O3 films. Journal of Physics and Chemistry of Solids, 2014, 75, 1201-1204.	4.0	73
6	Phase transformation and nanograin refinement of silicon by processing through high-pressure torsion. Applied Physics Letters, 2012, 101, .	3.3	65
7	Wide bandgap engineering of (GaIn)2O3 films. Solid State Communications, 2014, 186, 28-31.	1.9	63
8	Photocurrent induced by two-photon excitation in ZnTeO intermediate band solar cells. Applied Physics Letters, 2013, 102, .	3.3	61
9	Molecular beam epitaxial growth and optical properties of highly mismatched ZnTe1â^'xOx alloys. Applied Physics Letters, 2012, 100, .	3.3	60
10	Toward controlling the carrier density of Si doped Ga2O3 films by pulsed laser deposition. Applied Physics Letters, 2016, 109, .	3.3	60
11	Band alignment of Ga2O3/Si heterojunction interface measured by X-ray photoelectron spectroscopy. Applied Physics Letters, 2016, 109, .	3.3	52
12	Electrical properties of Si doped Ga2O3 films grown by pulsed laser deposition. Journal of Materials Science: Materials in Electronics, 2015, 26, 9624-9629.	2.2	51
13	Effects of dopant contents on structural, morphological and optical properties of Er doped Ga2O3 films. Superlattices and Microstructures, 2016, 90, 207-214.	3.1	47
14	Energy band bowing parameter in MgZnO alloys. Applied Physics Letters, 2015, 107, .	3.3	37
15	Regulation mechanism of bottleneck size on Li+ migration activation energy in garnet-type Li7La3Zr2O12. Electrochimica Acta, 2018, 261, 137-142.	5.2	37
16	Low temperature growth of europium doped Ga2O3 luminescent films. Journal of Crystal Growth, 2015, 430, 28-33.	1.5	36
17	Enhanced Light Output from ZnTe Light Emitting Diodes by Utilizing Thin Film Structure. Applied Physics Express, 2009, 2, 122101.	2.4	33
18	Fabrication of nanograined silicon by high-pressure torsion. Journal of Materials Science, 2014, 49, 6565-6569.	3.7	32

#	Article	IF	CITATIONS
19	Observation of low voltage driven green emission from erbium doped Ga2O3 light-emitting devices. Applied Physics Letters, 2016, 109, .	3.3	29
20	Lower temperature growth of single phase MgZnO films in all Mg content range. Journal of Alloys and Compounds, 2015, 627, 383-387.	5.5	28
21	Nanograin formation of GaAs by high-pressure torsion. Philosophical Magazine Letters, 2014, 94, 1-8.	1.2	27
22	Influence of substrate temperature on the properties of (AlGa)2O3 thin films prepared by pulsed laser deposition. Ceramics International, 2016, 42, 12783-12788.	4.8	27
23	Temperature dependence of luminescence spectra in europium doped Ga2O3 film. Journal of Luminescence, 2016, 177, 48-53.	3.1	26
24	Photogenerated Current By Two-Step Photon Excitation in ZnTeO Intermediate Band Solar Cells with n-ZnO Window Layer. IEEE Journal of Photovoltaics, 2014, 4, 196-201.	2.5	25
25	Realization of red electroluminescence from Ga2O3:Eu/Si based light-emitting diodes. Superlattices and Microstructures, 2021, 150, 106814.	3.1	25
26	Temperature dependence of Raman scattering in <i>\hat{l}^2</i> -(AlGa)2O3 thin films. AIP Advances, 2016, 6, .	1.3	24
27	Efficient pure green emission from Er-doped Ga ₂ O ₃ films. CrystEngComm, 2017, 19, 4448-4458.	2.6	23
28	Allotropic phase transformation and photoluminescence of germanium nanograins processed by high-pressure torsion. Journal of Materials Science, 2016, 51, 138-143.	3.7	21
29	Phase transformation of germanium by processing through high-pressure torsion: strain and temperature effects. Philosophical Magazine Letters, 2017, 97, 27-34.	1.2	21
30	Characteristics of thulium doped gallium oxide films grown by pulsed laser deposition. Thin Solid Films, 2017, 639, 123-126.	1.8	19
31	Aging and thermal stability of Mg/SiC and Mg/Y_2O_3 reflection multilayers in the 25–35 nm region. Applied Optics, 2005, 44, 5446.	2.1	18
32	Effect of VI/II ratio upon photoluminescence and electrical properties of phosphorus-doped ZnTe films grown by metalorganic vapor phase epitaxy. Thin Solid Films, 2011, 520, 743-746.	1.8	18
33	Electronic structure of GalnN semiconductors investigated by x-ray absorption spectroscopy. Applied Physics Letters, 2011, 98, .	3.3	18
34	Strategy toward white LEDs based on vertically integrated rare earth doped Ga2O3 films. Applied Physics Letters, 2021, 119, .	3.3	18
35	Toward the understanding of annealing effects on (Galn)2O3 films. Thin Solid Films, 2015, 578, 1-6.	1.8	16
36	The impact of dopant contents on structures, morphologies and optical properties of Eu doped Ga2O3 films on GaAs substrate. Journal of Luminescence, 2018, 194, 374-378.	3.1	16

#	Article	IF	CITATIONS
37	Yellow emission from vertically integrated Ga2O3 doped with Er and Eu electroluminescent film. Journal of Luminescence, 2021, 235, 118051.	3.1	16
38	Molecular beam epitaxial growth of ZnCdTeO epilayers for intermediate band solar cells. Journal of Crystal Growth, 2013, 378, 259-262.	1.5	15
39	Thermal annealing impact on crystal quality of (GaIn)2O3 alloys. Journal of Alloys and Compounds, 2014, 614, 173-176.	5.5	15
40	Influence of oxygen flow rate and substrate positions on properties of Cu-oxide thin films fabricated by radio frequency magnetron sputtering using pure Cu target. Thin Solid Films, 2019, 675, 59-65.	1.8	15
41	Band alignment of ZnTe/GaAs heterointerface investigated by synchrotron radiation photoemission spectroscopy. Applied Physics Letters, 2013, 102, 092107.	3.3	13
42	Improved Open-Circuit Voltage and Photovoltaic Properties of ZnTeO-Based Intermediate Band Solar Cells With n-Type ZnS Layers. IEEE Journal of Photovoltaics, 2017, 7, 1024-1030.	2.5	12
43	Structural properties of Eu doped gallium oxide films. Materials Research Bulletin, 2017, 94, 170-173.	5.2	12
44	Temperature-dependent Raman scattering in cubic (InGa)2O3 thin films. Journal of Alloys and Compounds, 2017, 690, 287-292.	5.5	12
45	Effect of oxygen flow rate on properties of Cu4O3 thin films fabricated by radio frequency magnetron sputtering. Journal of Applied Physics, 2020, 127, .	2.5	12
46	Effect of surface treatment on properties of ZnTe LED fabricated by Al thermal diffusion. Physica Status Solidi (B): Basic Research, 2006, 243, 959-962.	1.5	11
47	Crystal and electronic structural changes during annealing in severely deformed Si containing metastable phases formed by high-pressure torsion. Applied Physics Letters, 2018, 113, .	3.3	11
48	Cl-doping effect in ZnTe1-xOx highly mismatched alloys for intermediate band solar cells. Journal of Applied Physics, 2019, 125, 243109.	2.5	11
49	Epitaxial growth of (AlxGa1â^'x)2O3 thin films on sapphire substrates by plasma assisted pulsed laser deposition. AIP Advances, 2021, 11, 035319.	1.3	10
50	Pulsed laser deposition growth of ultra-wide bandgap GeO2 film and its optical properties. Applied Physics Letters, 2021, 119, .	3.3	10
51	Post-annealing effect upon phosphorus-doped ZnTe homoepitaxial layers grown by MOVPE. Physica Status Solidi (B): Basic Research, 2007, 244, 1634-1638.	1.5	9
52	Structural and optical properties of porous iron oxide. Solid State Communications, 2011, 151, 802-805.	1.9	9
53	Growth and characterization of Zn1-Cd Te1-O highly mismatched alloys for intermediate band solar cells. Solar Energy Materials and Solar Cells, 2017, 169, 1-7.	6.2	9
54	Ultraviolet emission from MgZnO films and ZnO/MgZnO single quantum wells grown by pulsed laser deposition. Journal of Crystal Growth, 2018, 483, 39-43.	1.5	9

#	Article	IF	CITATIONS
55	Efficient temperature sensor based on green emissions from Er-doped β-Ga2O3 thin film. AIP Advances, 2020, 10, .	1.3	9
56	Effects of oxygen gas pressure on properties of iron oxide films grown by pulsed laser deposition. Journal of Alloys and Compounds, 2013, 552, 1-5.	5.5	8
57	Development of ZnTe-Based Solar Cells. Materials Science Forum, 0, 750, 80-83.	0.3	8
58	Enhanced green emission from Er-doped (AlGa) ₂ O ₃ films grown by pulsed laser deposition. Japanese Journal of Applied Physics, 2020, 59, 051007.	1.5	8
59	Realization of rocksalt Zn _{1â^'x} Cd _x O thin films with an optical band gap above 3.0 eV by molecular beam epitaxy. CrystEngComm, 2020, 22, 2781-2787.	2.6	8
60	Low driven voltage green electroluminescent device based on Er:Ga2O3/GaAs heterojunction. Optical Materials, 2021, 116, 111078.	3.6	8
61	Growth characteristics of ZnMgTe layer on ZnTe substrate by metalorganic vapor phase epitaxy. Journal of Crystal Growth, 2007, 298, 449-452.	1.5	7
62	Growth and characterization of Fe3O4 films. Materials Research Bulletin, 2011, 46, 2212-2216.	5.2	7
63	Growth of InGaN layers on (1 1 1) silicon substrates by reactive sputtering. Journal of Alloys and Compounds, 2014, 587, 217-221.	5.5	7
64	Compositional dependence of optical transition energies in highly mismatched Zn _{1â^'} _x Cd _x Te _{1â^'} _y O _y alloys. Applied Physics Express, 2016, 9, 021202.	2.4	7
65	Photoluminescence and electrical properties of P-doped ZnTe layers grown by low pressure MOVPE. Journal of Crystal Growth, 2017, 468, 666-670.	1.5	7
66	Low temperature growth of Ga2O3 films on sapphire substrates by plasma assisted pulsed laser deposition. AIP Advances, 2019, 9, .	1.3	7
67	Three-dimensional band structure and surface electron accumulation of rs-CdxZn1â^'xO studied by angle-resolved photoemission spectroscopy. Scientific Reports, 2019, 9, 8026.	3.3	7
68	Low temperature growth of (AlGa)2O3 films by oxygen radical assisted pulsed laser deposition. CrystEngComm, 2020, 22, 142-146.	2.6	7
69	Improvement of sensing sensitivity based on green emissions from Er-doped (AlGa)2O3 films. Journal of Luminescence, 2021, 232, 117879.	3.1	7
70	Low threshold voltage blue light emitting diodes based on thulium doped gallium oxides. Applied Physics Express, 2021, 14, 081002.	2.4	7
71	Phosphorus-doped ZnMgTe bulk crystals grown by Vertical Bridgman Method. Physica Status Solidi C: Current Topics in Solid State Physics, 2006, 3, 812-816.	0.8	6
72	Post-annealing effect upon electrical and optical properties of MOVPE grown P-doped ZnTe homoepitaxial layers. Journal of Materials Science: Materials in Electronics, 2009, 20, 264-267.	2.2	6

#	Article	IF	CITATIONS
73	Growth of ZnTe layers on (111) GaAs substrates by metalorganic vapor phase epitaxy. Journal of Crystal Growth, 2012, 341, 7-11.	1.5	6
74	Epitaxial growth of ZnO layers on (111) GaAs substrates by laser molecular beam epitaxy. Thin Solid Films, 2012, 520, 2663-2666.	1.8	6
75	Effects of annealing treatment upon electrical and photoluminescence properties of phosphorus-doped ZnMgTe epilayers grown by metalorganic vapor phase epitaxy. Journal of Crystal Growth, 2013, 370, 342-347.	1.5	6
76	Study of Al thermal diffusion in ZnTe using secondary ion mass spectroscopy. Physica Status Solidi (B): Basic Research, 2007, 244, 1685-1690.	1.5	5
77	The impact of growth temperature on the structural and optical properties of catalyst-free <i>i²</i> -Ga ₂ O ₃ nanostructures. Materials Research Express, 2016, 3, 025003.	1.6	5
78	Photoluminescence of ZnTe/ZnMgTe multiple quantum well structures grown on ZnTe substrates by molecular beam epitaxy. Superlattices and Microstructures, 2018, 114, 192-199.	3.1	5
79	Nitrogen Doping Effect in Cu 4 O 3 Thin Films Fabricated by Radio Frequency Magnetron Sputtering. Physica Status Solidi (B): Basic Research, 2020, 257, 1900363.	1.5	5
80	Near-infrared light-emitting diodes based on Tm-doped Ga2O3. Journal of Luminescence, 2022, 245, 118773.	3.1	5
81	Faraday rotation measurement around Ni M2,3 edges using Al/YB6 multilayer polarizers. Journal of Electron Spectroscopy and Related Phenomena, 1999, 101-103, 287-291.	1.7	4
82	FARADAY AND MAGNETIC KERR ROTATION MEASUREMENTS ON Co AND Ni FILMS AROUND M2,3 EDGES. Surface Review and Letters, 2002, 09, 943-947.	1.1	4
83	Growth of boron-doped ZnTe homoepitaxial layer by metalorganic vapor phase epitaxy. Physica Status Solidi C: Current Topics in Solid State Physics, 2006, 3, 833-836.	0.8	4
84	Multilayer polarization elements and their applications to polarimetric studies in vacuum ultraviolet and soft X-ray regions. Nuclear Science and Techniques/Hewuli, 2008, 19, 193-203.	3.4	4
85	Fabrication of a ZnTe light emitting diode by Al thermal diffusion into a p-ZnTe epitaxial layer on a p-ZnMgTe substrate. Journal of Materials Science: Materials in Electronics, 2009, 20, 505-509.	2.2	4
86	Temperature dependence of electrical properties for P-doped ZnMgTe bulk crystals of high quality grown by Bridgman method. Journal of Crystal Growth, 2011, 318, 524-527.	1.5	4
87	Defect induced visible-light-activated near-infrared emissions in Gd3â^' <i>x</i> â^' <i>y</i> â^' <i>z</i> YbxBiyErzGa5O12. Journal of Applied Physics, 2017, 122, .	2.5	4
88	Effect of Nitrogen Doping on Structural, Electrical, and Optical Properties of CuO Thin Films Synthesized by Radio Frequency Magnetron Sputtering for Photovoltaic Application. ECS Journal of Solid State Science and Technology, 2021, 10, 065019.	1.8	4
89	Improved two-step photon absorption current by Cl-doping in ZnTeO-based intermediate band solar cells with n-ZnS layer. Solar Energy Materials and Solar Cells, 2022, 235, 111456.	6.2	4
90	MULTILAYER POLARIZERS FOR THE USE OF He-I AND He-II RESONANCE LINES. Surface Review and Letters, 2002, 09, 587-591.	1.1	3

#	Article	IF	CITATIONS
91	Fabrication of ZnO/ZnTe heterojunction by using a room temperature direct bonding technology. Physica Status Solidi C: Current Topics in Solid State Physics, 2014, 11, 1218-1220.	0.8	3
92	Highly transparent conductive Ga doped ZnO films in the near-infrared wavelength range. Journal of Materials Science: Materials in Electronics, 2016, 27, 9291-9296.	2.2	3
93	Growth properties of gallium oxide on sapphire substrate by plasma-assisted pulsed laser deposition. Journal of Semiconductors, 2019, 40, 122801.	3.7	3
94	Effects of Al doping on the structural, electrical, and optical properties of rock-salt ZnCdO thin films grown by molecular beam epitaxy. Journal of Physics and Chemistry of Solids, 2022, 163, 110571.	4.0	3
95	Strong enhancement of red photoluminescence from Eu doped Ga2O3 films by thermal annealing. Journal of Luminescence, 2022, 246, 118858.	3.1	3
96	Effect of gas flow rate on surface morphology and crystal quality of ZnTe epilayers grown on GaAs substrates. Materials Research Bulletin, 2011, 46, 551-554.	5.2	2
97	Surface morphologies and photoluminescence properties of undoped and P-doped ZnTe layers grown by metalorganic vapor phase epitaxy. Journal of Crystal Growth, 2013, 370, 348-352.	1.5	2
98	Impacts of oxygen radical ambient on structural and optical properties of (AlGa)2O3 films deposited by pulsed laser deposition. AIP Advances, 2020, 10, 065125.	1.3	2
99	Structural, optical, and electrical properties of WZ- and RS-ZnCdO thin films on MgO (100) substrate by molecular beam epitaxy. Journal of Alloys and Compounds, 2021, 867, 159033.	5.5	2
100	Improved photovoltaic properties of ZnTeO-based intermediate band solar cells. , 2018, , .		2
101	Impact of Radio Frequency Powers on GalnN Film Growth by Magnetron Reactive Sputtering. Japanese Journal of Applied Physics, 2012, 51, 118004.	1.5	2
102	Synchrotron radiation-excited etching of ZnTe using Ar gas. Nuclear Instruments & Methods in Physics Research B, 2005, 238, 115-118.	1.4	1
103	Temperature dependence of photoluminescence from Pâ€doped ZnMgTe bulk crystals of high quality grown by Bridgman method. Physica Status Solidi C: Current Topics in Solid State Physics, 2010, 7, 1495-1497.	0.8	1
104	Impact of Radio Frequency Powers on GalnN Film Growth by Magnetron Reactive Sputtering. Japanese Journal of Applied Physics, 2012, 51, 118004.	1.5	1
105	Epitaxial Growth of ZnTe Layers on ZnO Bulk Substrates by Metalorganic Vapor Phase Epitaxy. Japanese Journal of Applied Physics, 2013, 52, 040206.	1.5	1
106	Compositions of Mg and Se, surface morphology, roughness and Raman property of Zn1â^'Mg Se Te1â^' layers grown at various substrate temperatures or dopant transport rates by MOVPE. Journal of Crystal Growth, 2015, 414, 114-118.	1.5	1
107	Low pressure MOVPE growth and characterization of ZnTe homoepitaxial layers. Physica Status Solidi C: Current Topics in Solid State Physics, 2016, 13, 439-442.	0.8	1
108	Influence of source transport rate upon fractions of Mg and Se in Zn1-x Mgx Sey Te1-y layers grown by metalorganic vapor phase epitaxy. Physica Status Solidi C: Current Topics in Solid State Physics, 2016, 13, 443-447.	0.8	1

#	Article	IF	CITATIONS
109	Local Bi–O bonds correlated with infrared emission properties in triply doped Gd2.95Yb0.02Bi0.02Er0.01Ga5O12via temperature-dependent Raman spectra and x-ray absorption fine structure analysis. Journal of Physics Condensed Matter, 2018, 30, 125901.	1.8	1
110	Low temperature growth of In ₂ O ₃ films via pulsed laser deposition with oxygen plasma. Japanese Journal of Applied Physics, 2021, 60, 055505.	1.5	1
111	Creating terahertz pulses from titanium-doped lithium niobate-based strip waveguides with 1.55Âμm light. Journal of Materials Science: Materials in Electronics, 2021, 32, 23164-23173.	2.2	1
112	Characterization of epitaxial ZnTe layers grown on GaAs substrates by transmission electron microscopy and photoluminescence. Journal of Vacuum Science and Technology A: Vacuum, Surfaces and Films, 2012, 30, 021508.	2.1	0
113	Growth of ZnMgSeTe nearly lattice-matched to ZnTe and p-type doping by low-pressure MOVPE. Journal of Crystal Growth, 2017, 468, 671-675.	1.5	0
114	Conductive transparent (InGa)2O3 film as host for rare earth Eu. AIP Advances, 2020, 10, 025024.	1.3	0
115	Characterization of <i>p</i> -ZnTe/ <i>n</i> -ZnO Heterojunction Interface Prepared by Direct Bonding Technology. IEEJ Transactions on Electronics, Information and Systems, 2016, 136, 1761-1766.	0.2	0
116	Growth of low resistive Al-doped ZnCdO thin films with rocksalt structure for transparent conductive oxide thin films. , 2020, , .		0
117	Intermediate band solar cells based on highly mismatched II-VI oxide semiconductors. , 2020, , .		0
118	Low-temperature growth of In2O3 films on a-plane sapphire substrates by pulsed laser deposition. Thin Solid Films, 2022, 756, 139383.	1.8	0